Journal of Technical Physics, **20.** 2, 199-211, 1979.
Polish Academy of Sciences, Institute of Fundamental Technological Research, Warszawa.

DYNAMICS AND ADIABATIC POTENTIAL OF IMPURITY DEFECTS IN NEAR-SURFACE LAYER OF AB_2-TYPE STRUCTURES
PART I. SURFACE VIBRATION-MODES OF CRYSTALS WITH FLUORITE AND ANTIFLUORITE STRUCTURE

S. KACZMAREK and J. KAPELEWSKI (WARSZAWA)

1. Introduction

Crystals of fluorite structure (antifluorite being a fluorite form with reverse sublattice-valency), play a major role both in practice of quantum electronics and in a number of fields of physics as well as technology of solid bodies.

The variety of applications of this type crystals is linked with the fact that the class of crystals under consideration includes, except for the molecular bonds, all the other types of bonds. In fact, besides the media of the MeF_2 type (Me — bivalent metal), there occur here numerous compounds of electropositive bivalent elements with tetravalent negative ones, e.g. Mg_2Si, Mg_2Ge, intermetallic compounds, e.g. $PtAl_2$, $PtGe_2$ and even alloys, e.g. Fe_3Al. The wide applicability of wafers, among other things, in electrophonics and physics of admixtured crystals is one of the reasons for the immediate interest of the problem of dynamics of the near-surface layer and, in particular, the surface vibration-modes of this type crystals. In the case of the above mentioned problems the thermal phonon-spectrum is one of the chief factors that determine the statistical and thermodynamic parameters of crystals, as well as, through the characteristic and the form of the spectrum line, the spectroscopic properties of crystalline impurities. In view of the applications it is essential to explore the region of the shorter waves as well.

The aim of the present study is to analyze this problem for the case of the surface (110), on the base of a model of central and localized interactions [6]. The application of the above model to the construction of the dynamic matrix, on the one hand, all properties of the phonon spectrum, resulting from the spatial symmetry of the medium, to be formulated, ensuring thereby the generality of the,considerations concerning the structure, as results from the very assumption, and not a concrete crystal. On the other hand, this application is justified by the nature of the actual action of the vast majority of the representatives of the class of media under consideration, minimizing, at the same time, the number of the tabulation parameters. For the cases, wherein the essential role in the bonds is played by their ionic component (MeF_2-series), the model used here, generally speaking, does not apply. The surface vibration-modes of the MeF_2-series crystals, are studied in the paper [4], in the description of a continuous dielectric medium. It should be emphasized,

however, that even for this type media, the results obtained in the present paper, are adequate to the region of higher values of $k\sim$ (among other things, to the spectral range of thermal phonons) and this region, as is known, can always be modelled by the effective local potential.

2. Equations of Motion and Boundary Conditions

The crystal lattice of the structure AB_2 under consideration, has the symmetry of the spatial group O^5_h. The atoms A (structural equivalents of Ca in fiuorite) form a plane-centered cubic lattice, whereas the atoms B (corresponding there to the lattice points F) — a plain cubic lattice with constant lattice twice less, in such a way, that the ambiance B of each lattice point A forms a cube, at the centre whereof is A, while each lattice point B is surrounded tetrahedrally by four atoms A (Fig. 1). Such a configuration causes the atoms B of the unit cell of the crystal to form two translatorily unequivalent sub-lattices (B^1, B^2) the ambiances whereof penetrate into each other through the operation of inversion.

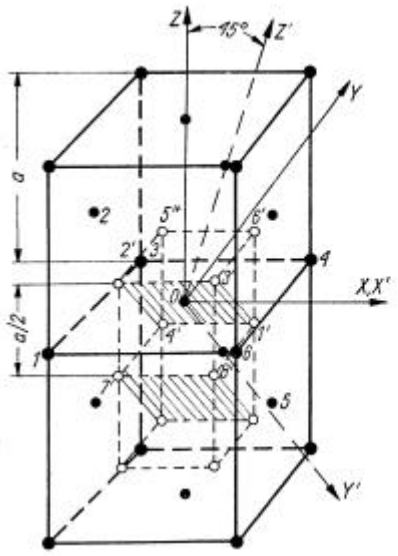

FIG. 1. Structure AB_2, lattice points *1-6* cone. *A;* 1'-*8'* lattice points *B* (wherein *1', 3', 5', 7'*- sublattice B^1; *2', 4', 6', 8'*—sublattice B^2).

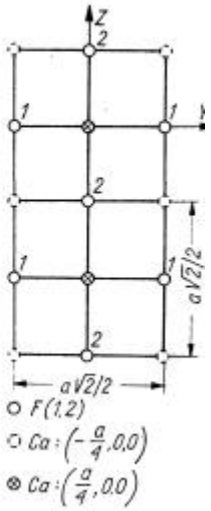

FIG. 2. AB_2 structure cross-section in *zy* plane.

The structure of the (110) section of the unit cell is depicted in Fig. 2, while that of the cross-sections in the planes normal to (110)—in Fig. 3. In the system of coordinates chosen here, the axis z is normal to the surface, while x and y coincide with the versors of translation in the (110) plane. From Fig. 3 it follows that both sublattice cease to be distinguishable in the case $k_x = 0$.

Since the basic contribution to the dynamic matrix is made by the action of the reverse-valency sublattice (see e.g. [2]), the equations of motion in the adopted model of actions, will be defined on the strength of the first coordination zone. In the notation of Fig. 1 they have the form:

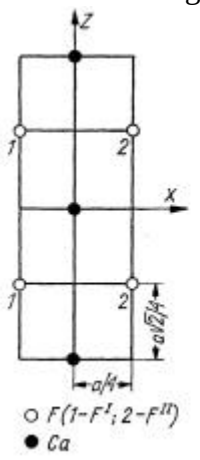

FIG. 3. AB_2 structure section in *zx* plane.

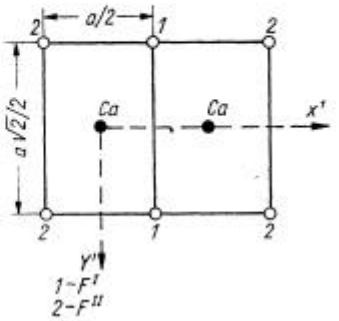

FIG. 4. AB_2 structure section in *xy-(110)* plane.

$$
\begin{aligned}
m_1 \frac{\partial^2 u^1(0)}{\partial t^2} &= \alpha[u^2(3')+u^2(1')+u^2(5')+u^2(7')+u^3(4')+u^3(2')+u^3(6') \\
&\quad +u^3(8')-8u^1(0)]+\beta[v^2(1')-v^2(3')+v^3(2')-v^3(4') \\
&\quad +\beta[-w^2(5')+w^2(7')+w^3(6')-w^3(8')], \\
m_1 \frac{\partial^2 v^1(0)}{\theta t^2} &= \gamma[v^2(1')+v^2(3')+v^3(2')+v^3(4')-4v^1(0)] \\
&\quad +\beta[-u^2(3')+u^2(1')+u^3(2')-u^3(4')], \\
m_1 \frac{\partial^2 w^1(0)}{\partial t^2} &= \gamma[w^2(5')+w^2(7')+w^3(6')+w^3(8')-4w^1(0)] \\
&\quad +\beta[-u^2(5')+u^2(7')+u^3(6')-u^3(8')], \\
m_2 \frac{\partial^2 u^2(1')}{\partial t^2} &= \alpha[u^1(0)+u^1(5)+u^1(4)+u^1(6)-4u^2(1')] \\
&\quad +\beta[v^1(0)-v^1(6)]+\beta[-w^1(5)+w^1(4)], \\
m_2 \frac{\partial^2 v^2(1')}{\partial t^2} &= \gamma[v^1(0)+v^1(6)-2v^2(1')]+\beta[u^1(0)-u^1(6)], \\
m_2 \frac{\partial^2 w^2(1')}{\partial t^2} &= \gamma[w^1(5)+w^1(4)-2w^2(1')]+\beta[-u^1(5)+u^1(4)], \qquad (2.1) \\
m_2 \frac{\partial^2 u^3(2')}{\partial t^2} &= \alpha[u^1(0)+u^1(1)+u^1(2)+u^1(3)-4u^3(2')]+ \\
&\quad +\beta[v^1(0)-v^1(3)]+\beta[w^1(1)-w^1(2)],
\end{aligned}
$$

$$m_2 \frac{\partial^2 v^3(2')}{\partial t^2} = \gamma[v^1(0)+v^1(3)-2v^3(2')]+\beta[u^1(0)-u^1(3)],$$

$$m_2 \frac{\partial^2 w^3(2')}{\partial t^2} = \gamma[w^1(1)+w^1(2)-2w^3(2')]+\beta[u^1(1)-u^1(2)],$$

$$\alpha = V''[r(1',0)]\frac{x^2(1',0)}{r^2(1',0)},$$

$$\beta = V''[r(1',0)]\frac{x(1',0)\cdot y(1',0)}{r^2(1',0)},$$

$$\gamma = V''[r(1',0)]\frac{y^2(1',0)}{r^2(1',0)},$$

$\bar{r}(1',0) = \bar{r}(1')-\bar{r}(0)$; m_1, m_2 — mass of the atoms A and B, u^i, v^i, w^i — components x, y, z of sublattice displacements

$$A(i=1), \quad B^1(i=2), \quad B^2(i=3).$$

The boundary conditions result from the comparison of the motion equations of the interior and the surface, and in the case under consideration reduce to the relationship.

$$\begin{aligned}
\alpha[u^2(7')+u^3(8')-2u^1(0)]+\beta[w^2(7')-w^3(8')] &= 0,\\
\gamma[w^2(7')+w^3(8')-2w^1(0)]+\beta[u^2(7')-u^3(8')] &= 0,\\
\alpha[u^1(5)+u^1(1)-u^2(1')-u^3(2')]+\beta[-w^1(5)+w^1(1)+w^2(1')-w^3(2')] &= 0,\\
\gamma[w^2(5)+w^1(1)-w^2(1')-w^3(2')]+\beta[-u^1(5)+u^1(1)+u^2(1')-u^3(2')] &= 0.
\end{aligned} \tag{2.2}$$

The central symmetry of actions ensures automatic fulfilment, in (2.1) and (2.2), of the conditions of translatory and rotational invariance of the crystal as a whole

$$\begin{aligned}
\sum_{\bar{l}} \Phi_{\alpha\beta}(\bar{l},\bar{l}') &= 0,\\
\sum_{\bar{l},\gamma} \Phi_{\alpha\beta}(\bar{l},\bar{l}')\varepsilon_{\beta\gamma\delta}X_\gamma(\bar{l}-\bar{l}') &= 0.
\end{aligned} \tag{2.3}$$

Should solely the wave be considered that propagates in the direction $y(k_x = 0)$, then by reason of the actual non-distinguishability of the two sublattices B, the relationships (2.1) and (2.2) undergo a simplification through eliminating the equations for (u^3, v^3, w^3) (they coincide then with the equations for (u^2, v^2, w^2)), as well as equating, in the remaining equations, the appropriate component deformations.

3. Solution to the Dynamic Problem of Surface

Substituting in the equations of motion (2.2) the deformation form characteristic of the surface modes:

$$\begin{bmatrix} u^r \\ v^r \\ w^r \end{bmatrix}(m,n,p) = \begin{bmatrix} u^r \\ v^r \\ w^r \end{bmatrix}(0,0,0)\exp[ik_1 m+ik_2 n-qp], \tag{3.1}$$

one obtains, on effecting a series of transformations, the characteristic equation $q(w))$ in the form:

$$\begin{vmatrix} F & G & H \\ G & K & L \\ H & L & M \end{vmatrix} = 0, \tag{3.2}$$

where

$$\begin{aligned}
F &= D - \frac{2}{E}\left\{\left[\mathrm{ch}^2 q\sqrt{2}/4 + \cos^2 k_2\sqrt{2}/4 + 2\mathrm{ch}\sqrt{2}q/4 \cdot \cos k_2\sqrt{2}/4 \cdot \cos k_1/2\right]\right. \\
&\qquad \left. + 2\left(2 - \cos^2 k_2\sqrt{2}/4 - \mathrm{ch}^2 q\sqrt{2}/4\right)\right\}, \\
K &= D - g\left(4\cdot\cos^2 k_2\sqrt{2}/4 + 2\sin^2 k_2\sqrt{2}/4\right), \\
M &= D - g\left[4\mathrm{ch}^2 q\sqrt{2}/4 + 2\left(1 - \mathrm{ch}^2 q\sqrt{2}/4\right)\right], \\
G &= g\sqrt{2}\cdot\sin k_2\sqrt{2}/4\cdot\mathrm{ch}\, q\sqrt{2}/4\cdot\sin k_1/2, \\
H &= g\sqrt{2}\, i\,\mathrm{sh}\, q\sqrt{2}/4\cdot\cos k_2\sqrt{2}/4\cdot\sin k_1/2, \\
L &= 2gi\cdot\mathrm{sh}\, q\sqrt{2}/4\cdot\sin k_2\sqrt{2}/4\cdot\cos k_1/2, \\
D &= 1 - \frac{m_1\omega^2}{8\alpha}, \\
g &= \left[4\left(1 - \frac{m_2\omega^2}{4\alpha}\right)\right]^{-1},
\end{aligned} \tag{3.3}$$

k_1, k_2 — components x, y of the wave vector $\bar{k}$, q — fading decrement, $i = \sqrt{-1}$.

The relationship (3.2) in an algebraic fourth-degree equation for chq, which yields, in general, 4 values of q that satisfy the condition of fading $Re\ q > 0$ and produce a general solution to the boundary problem in the form of the superposition:

$$\begin{bmatrix} u^r \\ v^r \\ w^r \end{bmatrix}(m, n, p) = \sum_{j=1}^{4} \begin{bmatrix} u_j^r \\ v_j^r \\ w_j^r \end{bmatrix}(0, 0, 0)\exp\left[ik_1 + ik_2 n - q_j p\right]. \tag{3.4}$$

On putting (3.4) into the boundary conditions (2.2) and expressing all the component amplitudes through $w^1(q_j) = w^1{}_j$; $(j = 1\text{-}4)$, one arrives at the set of equations:

$$\begin{aligned}
&\sum_{j=1}^{4}\left\{\frac{1}{2}\tilde{u}_j^1\cos k_1/4 - \frac{1}{\sqrt{2}}\, i\sin k_1/4 + \exp\left[-q_j\sqrt{2}/4\right]\left[\left(2\sqrt{2}\,\mathrm{ch}\, q_j\sqrt{2}/4\right.\right.\right. \\
&\quad \left.\left. + \sqrt{2}\,\mathrm{sh}\, q_j\sqrt{2}/4\right) i\sin k_1/4 + \sqrt{2}\tilde{v}_j^1\sin k_2\sqrt{2}/4\sin k_1/4 - \tilde{u}_j^1\left(\cos k_2\sqrt{2}/4\right. \\
&\quad \left.\left.\left. + \mathrm{ch}\, q_j\times\sqrt{2}/4 + 2\,\mathrm{sh}\, q_j\sqrt{2}/4\right)\cos k_1/4\right] g\right\} w_j^1 = 0,
\end{aligned} \tag{3.5}$$

$$\sum_{j=1}^{4}\left\{\frac{1}{2}\cos k_1 4 - \frac{i}{2\sqrt{2}}\tilde{u}_j^1\sin k_1/4 + \exp\left[-q_j\sqrt{2}/4\right]\left[\sqrt{2}\,\tilde{u}_j^1\left(\mathrm{sh}\, q_j\sqrt{2}/4\right.\right.\right.$$

(3.5) [cont.]

$$+\frac{1}{2}(\operatorname{ch} q_j\sqrt{2}/4-\cos k_2\sqrt{2}/4)\Big)\, i\sin k_1/4-(2\operatorname{ch} q_j\sqrt{2}/4+\operatorname{sh} q_j\sqrt{2}/4$$

$$+\tilde{v}_j^1\, i\sin k_2\sqrt{2}/4)\cos k_1/4\Big]g\Big\}w_j^1=0,$$

$$\sum_{j=1}^{4}\Big\{-\frac{1}{2}\tilde{u}_j^1\exp[-q_j\sqrt{2}/4]-[\tilde{u}_j^1(2\operatorname{sh} q_j\sqrt{2}/4-\operatorname{ch} q_j\sqrt{2}/4$$

$$-\cos k_2\sqrt{2}/4\cos k_1/2)+\sqrt{2}\,\tilde{v}_j^1\sin k_2\sqrt{2}/4\sin k_1/2]g\Big\}w_j^1=0,$$

$$\sum_{j=1}^{4}\Big\{-\frac{1}{2}\tilde{u}_j^1\exp[-q_j\sqrt{2}/4]-\Big[\operatorname{sh} q_j\sqrt{2}/4-2\operatorname{ch} q_j\sqrt{2}/4$$

$$+i\Big(\frac{1}{\sqrt{2}}\tilde{u}_j^1\cos k_2\sqrt{2}/4\sin k_1/2+\tilde{v}_j^1\sin k_2\sqrt{2}/4\cos k_1/2\Big)\Big]g\Big\}w_j^1=0,$$

$$\tilde{u}_j^1=(G_jL_j-H_jK_j)/(F_jK_j-G_j^2),\qquad \tilde{v}_j^1=(G_jH_j-F_jL_j)/(F_jK_j-G_j^2).$$

The determinant of the set (3.5) yields the dispersion dependence wanted.

4. Results of Numerical Calculations

The numerical results obtained by using the Odra 1305 computer are shown below (with the denotations:

$$\tilde{\omega}^2=\frac{m_1\omega^2}{8\alpha},\qquad R=m_1/m_2).$$

From the plots obtained the following general conclusions can be drawn:

1. For the range R explored (including the two variations i.e. fluorite and antifluorite) the surface modes occur on both the acoustic and the optic branch nearly throughout Brillouin's zone (see below), except that in the case $k_y = 0$ (for which the two sublattices B are non-distinguishable) there occur two optical branches (Figs. 5,9) while in the remaining cases,— one (Figs. 7, 14). The parabolic character obtained here $w^2(k)$ in the region of small k for the acoustic branch, corresponds to the linear dependence for $w(k)$.

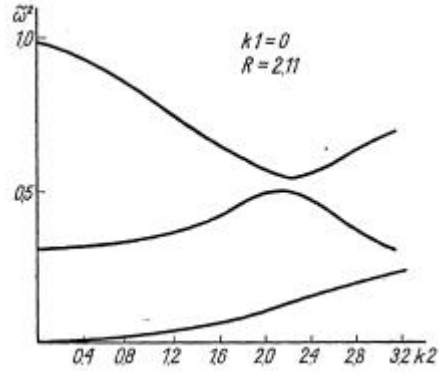

FIG. 5. Dispersion curves w^2 (0; k_2), R = 2.11 (CaF_2).

2. In the first half of Brillouin's zone the dispersion relationship for the acoustic branch shows one maximum and one minimum, the positions whereof do not depend upon the ratio of masses R (it is only the frequency value at the maximum point that depends upon this ratio). At the minimum points and their nearest surroundings $Re\ q = 0$, consequently these are the only regions wherein the surface mode does not exist (Fig. 21). The conclusions discussed concern Figs. 6, 10, 11 -17.

3. The value of the above-mentioned maximum as well as the phase velocity (for the

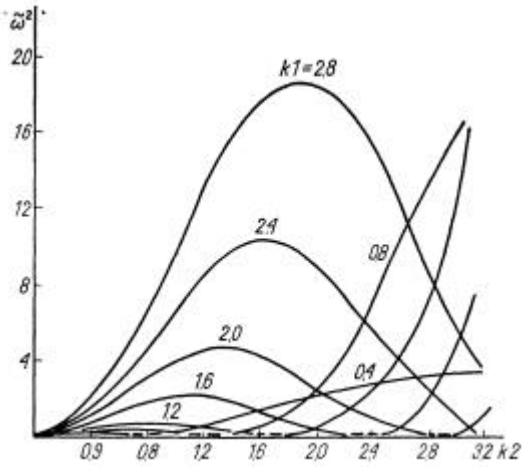

FIG. 6. Family of dispersion curves $w^2\ (k_1; k_2)$ for various values of k_1 (acoustic branch), R = 2.11.

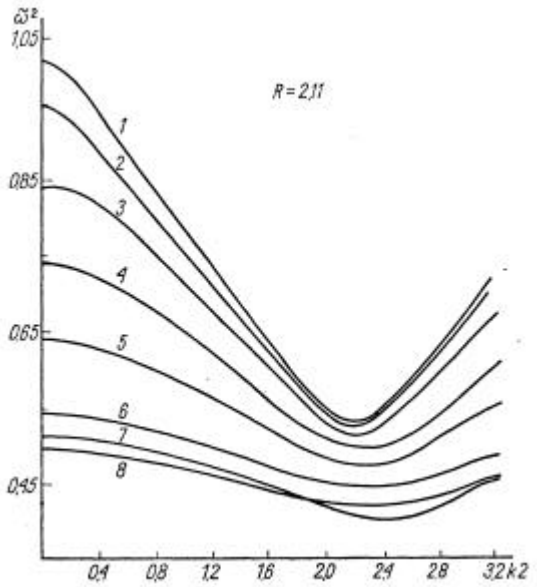

FIG. 7. Family of dispersion curves $w^2\ (k_1; k_2)$ for various values of k_1 (optical branch), R =2.11. Curves 1-8 for k_1 = 0; 0,4; 0.8; 1.2; 1.6; 2.0; 2.4.

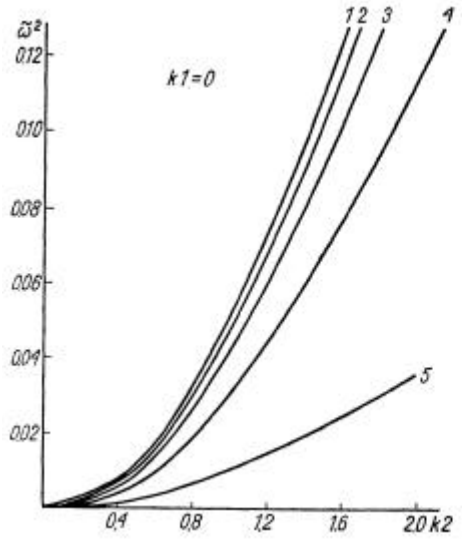

FIG. 8. Dispersion curve w^2 (0; k_2) (acoustic branch). Numbers *1-5* correspond, respectively, to: R= 10; 7.23; 4.61; 2.11; 0.4.

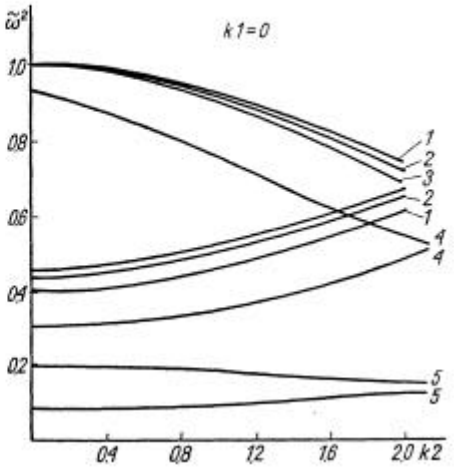

FIG. 9. Dispersion curve w^2 (0; k_2) (acoustic branch) Notat. see Fig. 8.

given *R)* grow with the increase *of* k_x (for the given k_y), With the increase k_x the maximum shifts towards the greater k_y (Fig. 6).

4. With the increase of $m_2(m_2 = m(B))$ (at steady-state m_1) the frequency and the phase velocity of vibration both acoustic and optical, decreases (Figs. 7 - 13).

5. In the first half of the Brillouin's zone the frequency and the phase velocity of the optical vibration decrease with the increase of *kx* (for the given k_y) (Figs. 7, 14).

6. The fading decrements show a slight dependence upon *R.* This conclusion concerns both branches (Figs. 19, 20).

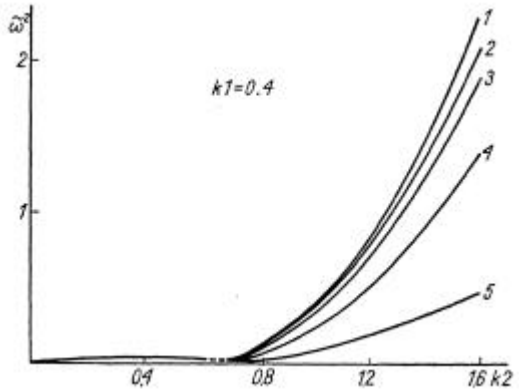

FIG. 10. Dispersion curve w^2 (0.4; k_2) (acoustic branch) Notat. see Fig. 8.

7. Within the boundary k -> 0, for the optical branch, the fading decrements (dimen-sionless i.e. $q = \beta \cdot a$) attain the value of the order 1 (i.e. $\beta \sim a^{-1}$). Consequently the optical vibrations fade with the distance from the surface.

8. The dispersion relationships obtained, presented here for selected values of R, permit the dependence $\omega^2(k)$ to be plotted for an arbitrary R, with no additional calculations being performed (Figs. 15 -18).

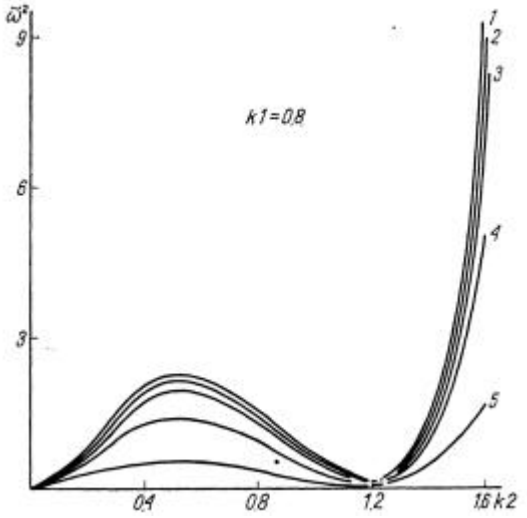

FIG. 11. Dispersion curve ω^2 (0.8; k_2) (acoustic branch), Notat. see Fig. 8.

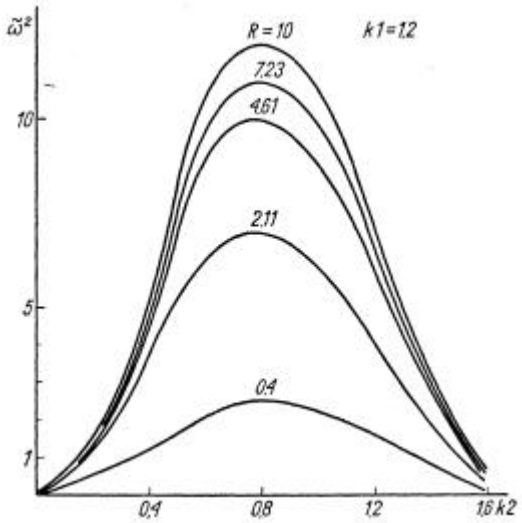

FIG. 12. Dispersion curve $\omega^2(1.2; k_2)$ (acoustic branch).

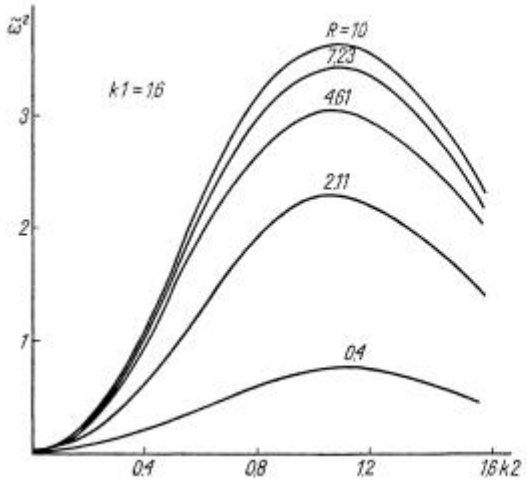

FIG. 13. Dispersion curve w^2 (1.6; k_2) (acoustic branch).

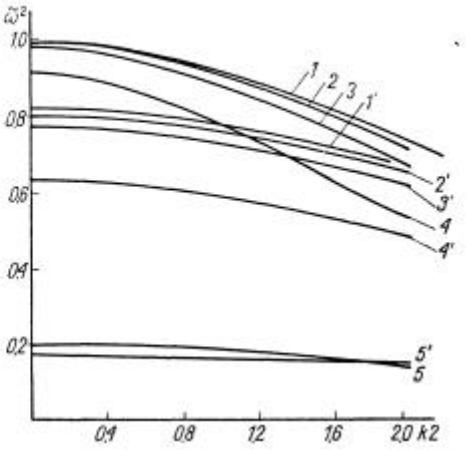

FIG. 14. Dispersion curves optica vibration w^2 (0.4; k_2)-(l-5) as well as (1.6; k_2) – *(1'-5')*. Notat. see Fig. 8.

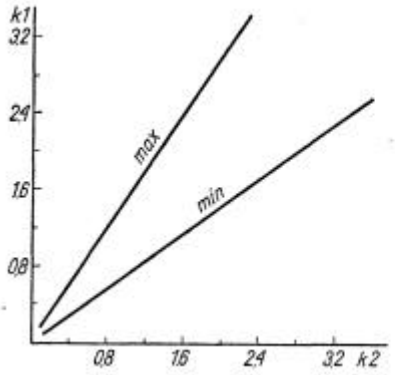

FIG. 15. Position of local extreme points in the first half of Brillouin's zone in the k plane.

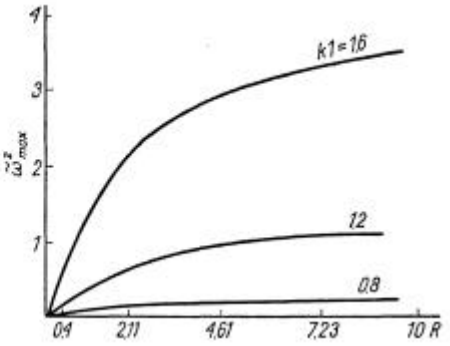

FIG. 16. Dependence of local-maximum value of o w^2 upon R for various k_1.

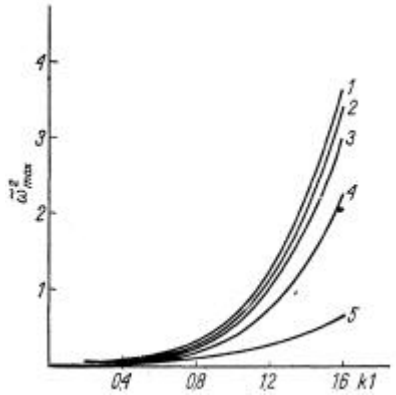

FIG. 17. Local-maximum value of w^2 in function of k_1 for various R. Notat. see Fig. 8.

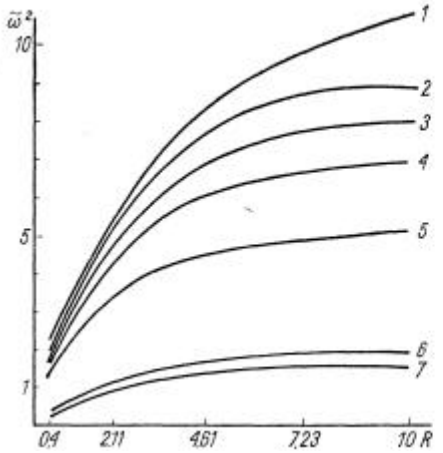

FIG. 18. Change in $\tilde{w}^2$ $(k_1; k_2)$ depending upon R (acoustic branch). The curves *1-7* correspond, respectively, to: $k_1 = 1.6; k_2 = 0.4$; $k_1 = 0.8; k_2 = 1.6; k_1 = 0.4; k_2 = 1.2; k_1 = 1.2; k_2 = 1.2; k_1 = 1.2; k_2 = 0.4; k_1 = 0.8; k_2 = 0.4; k_1 = 0.8; k_2 = 0.8$.

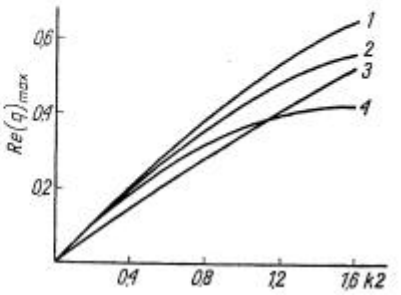

FIG 19. Dependence of maximum decaying -decrement upon wave vector (acoustic branch), curves *1-4* correspond, respectively, to $k_1 = 0.4$; 0.8; 1.2; 1.6 and do not depend upon R,

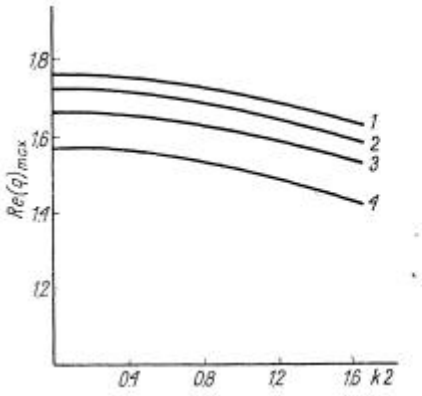

FIG. 20. Dependence of maximum decaying-decrement upon wave vector (optical branch). Notat. see Fig. 19.

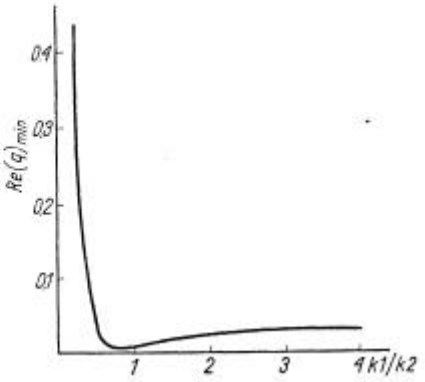

FIG. 21. Dependence of minimum decay ingrement upon k_1/k_2 ratio for the acoustic branch

5. Concluding Notes

The results presented testify to the existence of the surface vibration modes of the fluorite-structure lattice on both the acoustic and the optical branch, independently of the mass ratio of the two components. The results permit also, in the region of the actual locality of the dynamic matrix, both the dispersion relationships and the dependence of decaying decrements upon the wave vector, to be determined, for, practically, any representative to the structure under consideration.

The above remark concerns in particular the spectra of the thermal phonons in MeF_2 and in this connection is of primary practical importance also in the analysis of a number of physical processes in the boundary layer and its interactions with the electrons of admixtures which enables, among other things, its thermodynamic parameters, the width and form of the spectral line of near-surface paramagnetic impurities, acoustic resonance and the like [6], to be calculated.

A strictly near-surface nature of vibration on the optical branch, as demonstrated in this paper, characterizes the dynamics of this fragment of lattice and constitutes from the above angle a substantial element that influences a number of materials properties of the boundary layer.

References

1. R. SRINIVASAN, Phys. Rev., 165, 1054, 1968.
2. Z. IWANIENKO, B. MALKIN, F.T.T, **11,** 7, 1969.
3. S. KALISKI, J. KAPELEWSKI, **Cz.** RYMARZ, Arch. Mech., 23, 6, 1971.
4. **W. BRYKSIN, J.** GERBSTEIN, D. MIRLIN, **F.T.T., 14,** 11, 1972.
5. A. MARADUDIN, J. MELNGAILIS, Phys. Rev., 133, 4A, 1964.
6. A. MARADUDIN, E. MANTROLL, G. WEISS, *Theory of lattice dynamics in the harmonic approximation*, New York-London 1963.
7. S. GANESAN, R. SRINIVASAN, Can. J. Phys., **40,** 74, 1964.
8. B. MALKIN, F.T.T., **11,** 5, 1969.
9. M. BORN, H. KUN, *Dynamical theory of crystal lattices,* Oxford 1954. 10. A. KELLY, G. GROVES, *Crystallography and crystal defects,* London 1970.

Streszczenie

DYNAMIKA I POTENCJAL ADIABATYCZNY DEFEKTÓW DOMIESZKOWYCH W WARSTWIE PRZYPOWIERZCHNIOWEJ STRUKTUR TYPU AB_2
CZ. I. POWIERZCHNIOWE MODY DRGAÑ KRYSZTA£ÓW 0 STRUKTURZE FLUORYTU I ANTYFLUORYTU

W pracy rozwi¹zano problem powierzchniowych modów drgañ kryszta³ów o strukturze fluorytu i antyfluorytu i powierzchni (110), na podstawie modelu oddzia³ywañ centralnych i zlokalizowanych.

Podano relacje dyspersyjne oraz określono charakter zmienności dekrementów zanikania obu ga³êzi dla ró¿nych wartości stosunku mas sk³adników komórki elementarnej.

Uzyskane wyniki s¹ szczególnie efektywne w opisie procesów z udzia³em fononów termicznych warstwy brzegowej.

Ðåçþìå

ÄÈÍÀÌÈÊÀ È ÀÄÈÀÁÀÒÈ×ÅÑÊÈÉ ÏÎÒÅÍÖÈÀË ÏÐÈÌÅÑÍÛÕ ÄÅÔÅÊÒÎÂ Â ÏÐÈÏÎÂÅÐÕÍÎÑÒÍÛÕ ÑÒÐÓÊÒÓÐ ÒÈÏÀ À A_2 ×. I. ÎÏÅÐÕÍÎÑÒÍÛÅ ÏÎÄÓ ÊÎÅÁÀÍÈÉ ÊÐÈÑÒÀËËÎÂ **ÑÎ** *ÑÒÐÓÊÒÓÐÎÉ ÔÉÞÏÐÈÒÀ È ÀÍÒÈÔÉÞÏÐÈÒÀ*

Â ðàáîòå ðàññìàòðèâàþòñÿ ìîäåëè ïîâåðõíîñòíûõ ìîäîâ êîëåáàíèé êðèñòàëëîâ ñî ñòðóêòóðîé ôëþîðèòà è àíòèôëþîðèòà è ïîâåðõíîñòè (110), îí èðàñ íà ìîäåëü öåíòðàëüíûõ è ëîêàëèçèðîâàííûõ âçàèìîäåéñòâèé.

Ï ðèâåäåíû äèñïåðñèîííûå ñîîòíîøåíèÿ è îï ðåäåëåí õàðàêòåð èçìåíåíèÿ äâóõ âåòâåé çàòóõàíèÿ îêîëî ïîâåðõíîñòíîãî ýêñèòîíà, äëÿ ðàçíûõ çíà÷åíèé îòíîøåíèÿ ìàññ êîìïîíåíò ýëåìåíòíîé ÿ÷åéêè.

Ï îêó÷åíûå ðåçóëüòàòû îñîáåííî ýôôåêòèâíû â îïèñàíèè ï ðîöåññîâ ñ ó÷àñòèåì òåí ëîâûõ ôîíîíîâ ãðàíè÷íîãî ñëîÿ.

Received Ì àð*14, 1978.*